



ANP-10263Q1NP
Revision 0

Response to Request for Additional Information

**ANP-10263P, Codes and Methods Applicability Report for the
U.S. EPR**

March 2007

AREVA NP Inc.

Non-Proprietary

**Response to Request for Additional Information – ANP-10263P
“Codes and Methods Applicability Report for the U.S. EPR” (TAC No. MD2803)**

NRC Comment

Validation of Methodology for Small Break LOCA

The vertical and horizontal flow maps in S-RELAP5 are described in Section 3.1 of R1. Interphase friction is described in Section 3.2 of R1 (see references below), including entrainment. The models have been assessed by AREVA and have been found acceptable for SBLOCA evaluations.

The EPR relies on steam generator crash cooling (including reflux condensation) to bring the primary system pressure down to the cutoff head of the medium head safety injection (MHSI) system pumps during SBLOCAs. The main steam relief train (MSRT) is used to depressurize the SG at a rate of 180°F/hr, and is actuated following an SI signal. The MSRT is also used to manage an STGR event.

RAI 1: *The description of the automatic depressurization method presented in ANP-10276 is clearer. The cooling rate is only an approximation of the process which is a pressure set-point reduction over a period of time. ANP-10263P should be modified to clarify this method.*

Response 1:

The following changes will be made to the topical report ANP-10263P when it is issued as an approved report in order to clarify the information.

Modification to Section 2.1.2.2 Secondary Side OPP, page 2-7

The third bullet of the second paragraph will be replaced with the following:

- During certain accidents (e.g., SBLOCA), the Main Steam Relief Trains (MSRTs) are used to depressurize and cool the secondary side. Upon a low-low pressurizer, pressure safety injection signal, the steam generator secondary side is depressurized to 870 psia. The depressurization rate is controlled by changing the secondary pressure setpoint of the MSRT from the post-trip setpoint (nominally 1385 psia) to 870 psia in approximately 20 minutes. This depressurization reduces secondary side saturation temperature at 180 °F/h. The reduction in the secondary side temperature cools and depressurizes the primary system to facilitate adequate injection from the MHSI system.

Modification to Section 4.1.2 Small Break LOCA Scenarios, page 4-4

The second paragraph in this section will be replaced with the following paragraphs:

The SIS is actuated on very low (low-low) PZR pressure. The SI signal automatically starts the MHSI and LHSI pumps (the U.S. EPR does not have HHSI pumps) and initiates a partial cooldown of the secondary system. The partial cooldown cools the primary system and lowers RCS pressure sufficiently to enable the injection of MHSI water into the cold legs.

The partial cooldown is performed by all SGs using the MSRTs. The MSRTs depressurize the SGs at a controlled rate by changing the secondary pressure setpoint of the MSRTs from the post-trip setpoint (nominally 1385 psia) to 870 psia in approximately 20 minutes. This depressurization results in a reduction in secondary saturation temperature at 180 °F/h. The accompanying reduction in RCS pressure is low enough to enable the needed MHSI injection while still high enough to prevent core recriticality.

NRC Comment

The U.S. EPR SG design includes an economizer, a feedwater preheating section (Figure 2-5 does not appear to show this feature).

RAI 2: *Provide a better pictorial representation of the economizer, both elevation and cross-section views, either replacement or additional figure. On modeling Figure 5-2, provide a cross-section view showing the economizer modeling.*

Response 2:

The following changes will be made to the topical report ANP-10263P when it is issued as an approved report in order to clarify the information.

Modification to Section 2.1.1 Reactor Coolant System, page 2-2

An additional sentence will be added at the end of the second paragraph in this section:

“Figure 2-5a illustrates the concept and operation of the SG axial economizer.”

The new Figure 2-5a follows this response.

Revised Figures 5-2 and C-2

The figures will be modified to include a cross-section view of the economizer modeling. The revised figures follow this response.

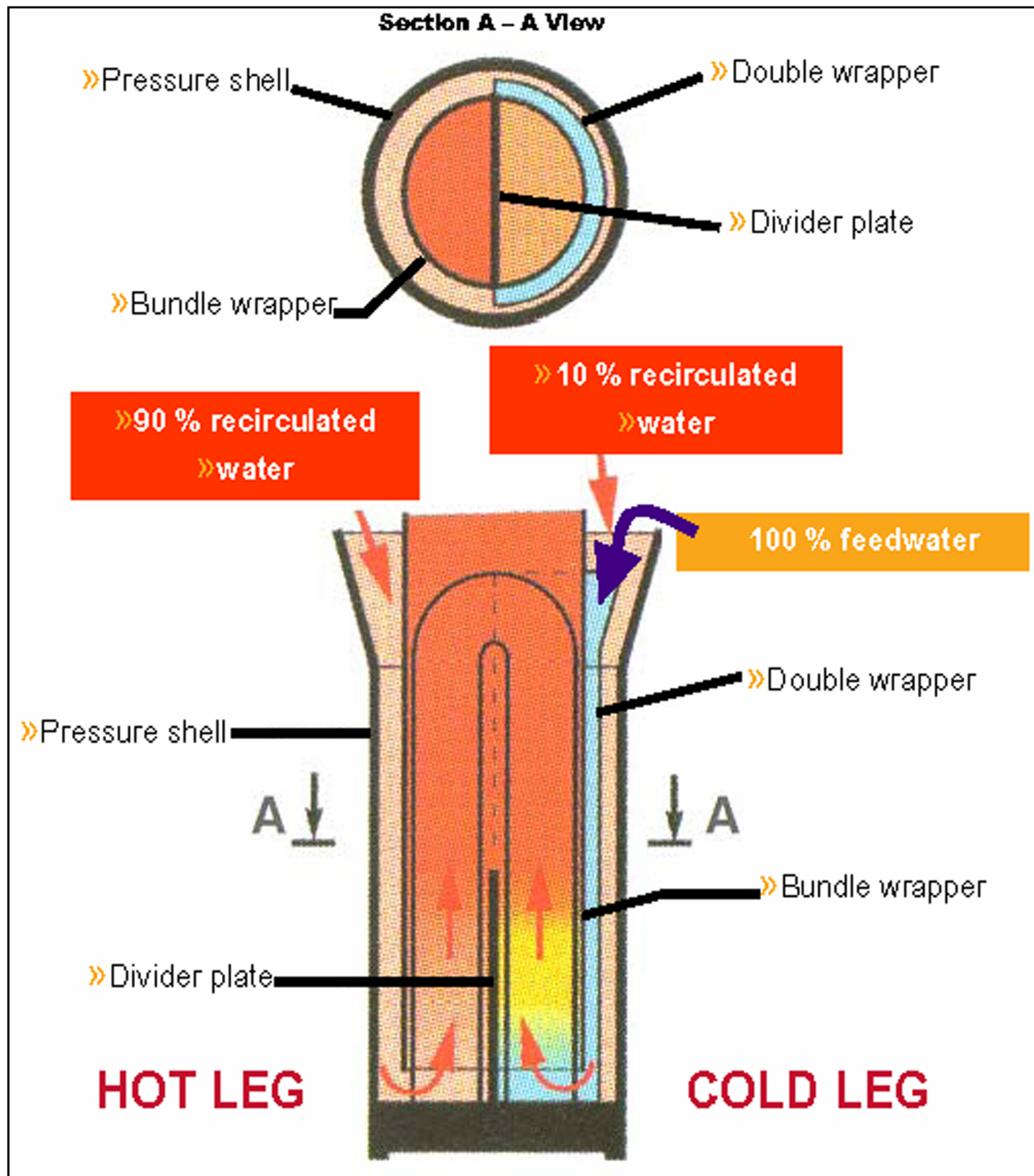


Figure 2-5a
Steam Generator Axial Economizer

Figure 5-2 U.S. EPR Secondary Side Nodalization

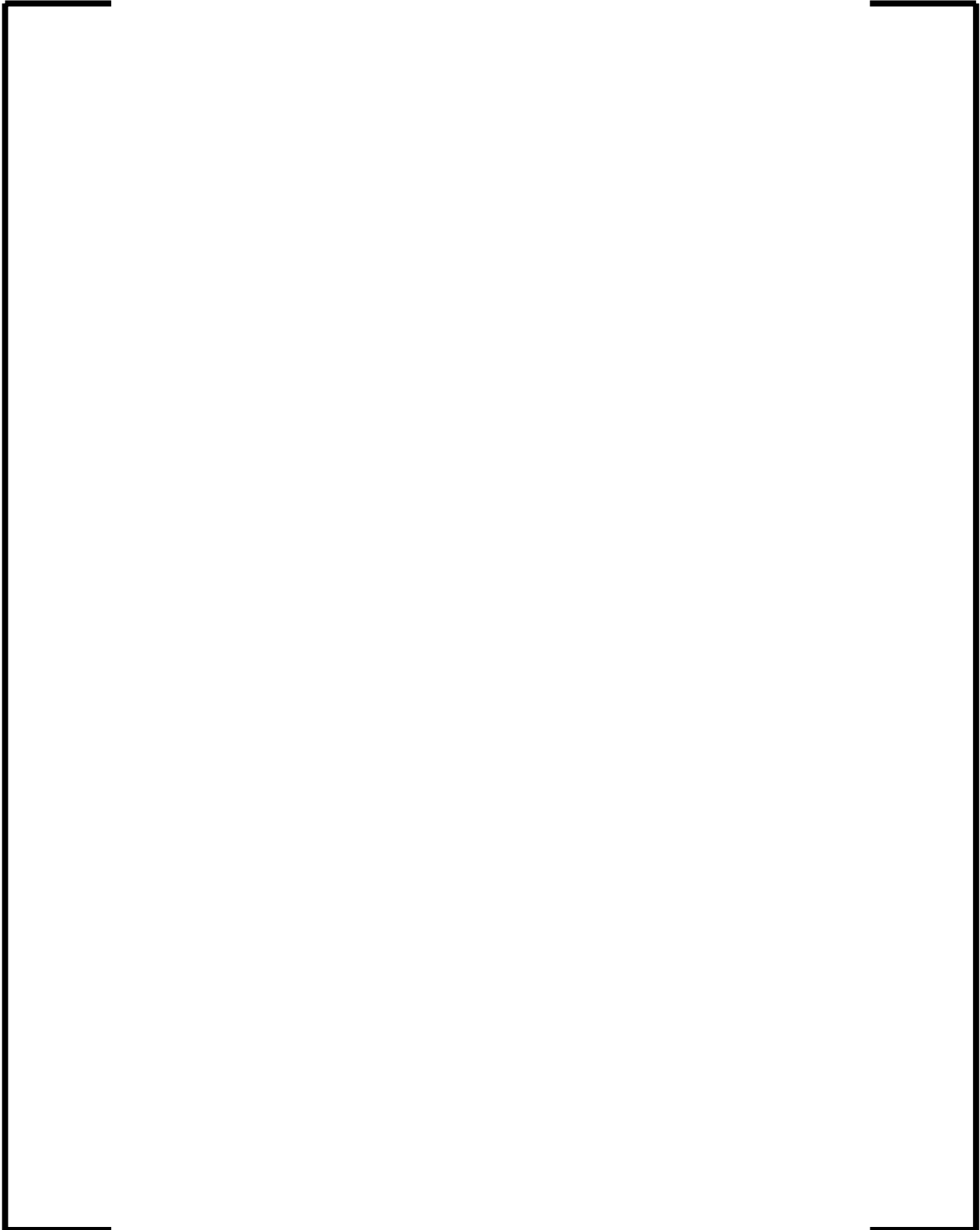
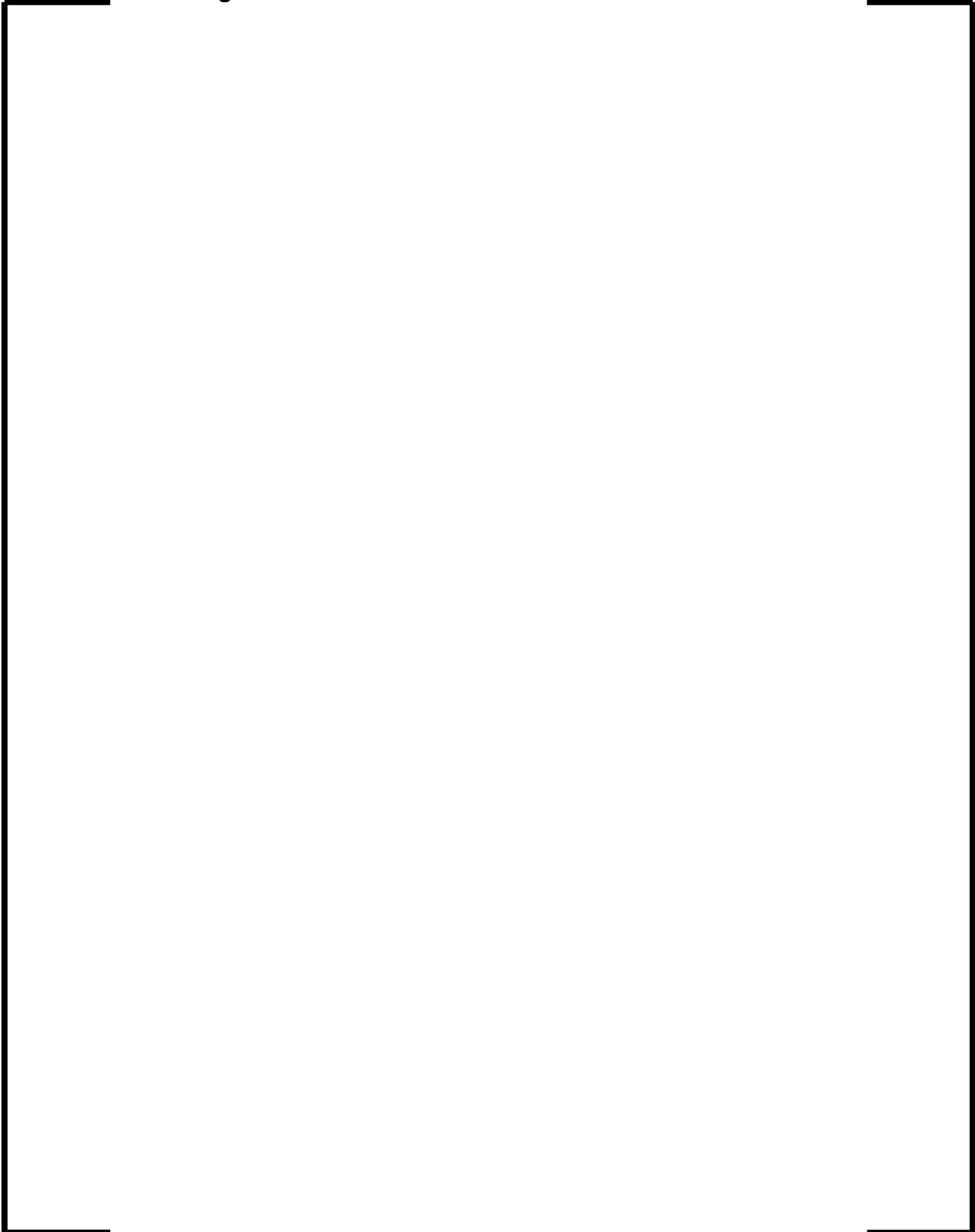


Figure C-2 U.S. EPR Steam Generator Nodalization



NRC Comment

AREVA used BETHSY test 9.1.b (R2) to evaluate the MHSI system (R3). It is also noted that the assessment for loop seal clearing used BETHSY as well as UPTF-A5RUN11E (R3). There is no mention of any adjustment to the physical loop seal model for UPTF in R3, "behavior is not particularly sensitive" to nodalization or time step. However, for BETHSY, an artificial adjustment was made based on observed results from the test. This adjustment carries over to the SBLOCA methodology.

RAI 3: *Did the UPTF S-RELAP5 model include a bias in the loop seal? If so, the modeling description should be modified.*

Response 3:

The S-RELAP5 model of the UPTF loop seal did not include the bias. This test was used to assess the interphase drag in the loop seal during transition between horizontal slug and horizontal stratified flow.

RAI 4: *Justify the bias in BETHSY as the correct method to address the observed uncertainties in the break flow rate, the uncertainties in the auxiliary feedwater flow control logic, and the uncertainties in predicting the flow regime in the U-tubes (water hold-up), which could also influence loop-seal clearing in a loop. These uncertainties could all be related to the calculated performance of the SGs and the resulting uncertainties in the RCS pressure and temperature.*

Response 4:

The uncertainties in break flow rate, auxiliary feedwater flow control logic, and the uncertainties in predicting the flow regime in the U-tubes (which could all affect the loop-seal clearing in a loop) are not intended to be addressed by the loop seal biasing. As the reviewer states, the above uncertainties are related to the calculated performance of the steam generators and the resulting uncertainties in the system pressure and temperature. The loop seal biasing methodology was not developed based on the BETHSY assessment. The loop seal biasing methodology was developed prior to the BETHSY assessment and was applied to the assessment so that the experimentally observed loop would clear in the S-RELAP5 calculation. The results from the BETHSY assessment demonstrate that the strategy performed as designed and that the loop seal clearing process and post-clearing behavior in the test were well predicted.

NRC Comment

Little information could be located concerning the scope of modeling studies of the SGs, beyond the number of axial nodes used to model the U-tubes. However, the effects of nodalization have been shown to influence the analytical results, R4.

Of particular concern, because of the importance of using the SGs to manage design basis accidents, is the treatment of the U-tubes which have varying tube lengths. There are a number of tests which show non-uniform conditions exist in the tube bundles.

Tests have shown the following:

- 1. Non-uniform flow conditions can be expected in the steam generator during reflux condensation. Some tubes may be in a condensing co-current two-phase flow pattern while others stagnate. This has been found to cause a reduction in the effective heat transfer area in the SG. (R5, R6, R7, R8 and R9)*
- 2. Noncondensable gases can accumulate in the U-tubes. These noncondensables can originate from air initially dissolved in the primary coolant. Local condensation heat transfer coefficients are known to decrease as the noncondensable gas mass fraction increases (R10 and R11).*
- 3. Secondary transient depressurization in one ROSA test (R11) was found to cause a significant relocation of the primary mass. Condensate accumulated in the crossover leg as well as in the SG tubes of the affected loop. Reactor pressure vessel mass decreased during this time, and core dryout progressed until it was later slowed by an increase in the reflux flow rate.*

RAI 5: *Provide additional nodalization and test comparison analyses to fully qualify the S-RELAP5 heat and mass transfer package for modeling the EPR SG performance during small-break LOCAs, including an STGR. These studies are to include both axial nodalization as well as multiple U-tube paths to address the observed non-uniform flow conditions, and the modeling of the U.S. EPR economizer. The results of these studies will be used to justify the S-RELAP5 model to be used for licencing analyses.*

RESPONSE 5:

SG nodalization studies will be performed for the BETHSY facility, SBLOCA test 9.1b. The results of the study will be used to justify the S-RELAP5 model used for licensing analyses.

BETHSY is a scaled down model of a 900 MWe (2775 MWth) Framatome 3-loop PWR. The facility is 1/100 volumetric scaled with one-to-one elevation scaling.

BETHSY Test 9.1b simulated a 0.5% cold leg break (2 inch equivalent) with High pressure Injection System (HPIS) failure. This led to a large core uncover and fuel heatup, and resulted in the implementation of a rapid depressurization of the secondary system initiated when the maximum heater rod cladding temperature reaches 450 °C. As a result of this secondary system depressurization, the primary system depressurized allowing the accumulators and eventually the Low Pressure Injection System (LPIS) to inject and recover the core.

This test was chosen for the study to be performed in response to this question because it was part of S-RELAP5 benchmarking tests and because, like the U.S. EPR, the SG is depressurized to allow for low pressure ECCS injection.

Sensitivity studies of axial nodalization in the SG tubes and of multiple U-tube paths will be performed prior to submittal of the DCD. Each SG in the BETHSY facility has 34 U-tubes. Two paths will be modeled:

- the short U-tubes with 18 tubes of lengths varying from 9.139m to 9.552m
- and the long U-tubes with 16 tubes of lengths varying from 10.299m to 10.6782m.

The average length of the tubes will be calculated as follows:

$$L_{avg} = (\sum L_n * N_{tubes \text{ of length } L}) / \text{Number of tubes in region}$$

The results of these sensitivities will be used to justify the model for the U.S. EPR. If the results of the study indicate that the nodalization should be changed for the U.S. EPR, then the analysis for the DCD will be performed with the revised nodalization.

The SGTR will not be addressed as part of this study since loop seal clearing and different U-tube behavior are not important phenomena in the SGTR event. The SGTR nodalization models the ruptured tube (or tubes) as a separate path.

RAI 6: *Section 4.2.5 - It is not clear if it will be acceptable to terminate the calculation when the fuel temperature transient in the core has been reversed. How does this relate to the description presented in Section 4.1.1 for the length of the calculation? Justify this in consideration of the requirement to demonstrate acceptable cladding oxidation and core cooling if there are prolonged periods of high cladding temperatures.*

RESPONSE 6:

The SBLOCA sample problem was performed up to a time when the temperature was sufficiently low to conclude that the PCT had occurred and that the total oxidation would not increase significantly past this time. In order to provide further assurance of this conclusion, the analysis for the DCD will be performed until the top of the active fuel has been covered with a two-phase mixture and the cladding temperatures have been reduced to temperatures near the saturation temperature.

Validation of S-RELAP5 Methodology for Non-LOCA Events

RAI 7: *Section C.2, page C-3: It is not clear where the 1406.9 psia value comes from, the graphical output does not reach this value. The post-trip set-point for the MSRT is not this high. Where does this value come from? Modify the text, or graphical output, according.*

Response 7:

The MSRT system is composed of two valves in series: a normally closed, very fast opening Main Steam Relief Isolation Valve (MSRIV) and a normally open, slow moving motor-operated Main Steam Relief Control Valve (MSRCV). The MSRIV opens when the pressure in the steam generator first exceeds the MSRT control setpoint.

Following a LOCA safety injection signal, the MSRT pressure control setpoint is reduced from nominally 1385.1 psia (+ 21.8 psia uncertainty = 1406.9 psia) to 870 psia (+ 22 psia uncertainty = 892 psia) at a rate corresponding to a reduction in the saturation temperature of 180 °F/h. This reduction in setpoint occurs whether the MSRIV has opened or not. Therefore, depending on the length of time elapsed from the start of cooldown and the rate that secondary pressure rises, the MSRIV may open at a pressure that is much lower than 1385.1 psia. The reduction in pressure control setpoint proceeds independently of actual secondary side pressure.

In the sample problem, SG1 secondary pressure intersects the cooldown curve at 70.8 seconds at a SG1 pressure of 1382 psia and the MSRIV opens. The opening of the valve results in a high flow through the MSRCV (which at that time is 100% open) and a drop in SG pressure of about 120 psia resulting in MSRCV modulating close. The MSRCV modulates open again at 206 seconds at a pressure in SG of 1316.1 psia. From then on the SG pressure follows the cooldown curve. Figure 7-1 presents this behavior for SG1. The other three SGs behave similarly.

The MSRCV is fully open during plant operation at 100% thermal power. As thermal power decreases, the valve closes proportionately down to a minimum of 40% capacity. The closure of the valve on thermal power was not modeled in the sample problem. The valve closes entirely whenever secondary pressure falls below the MSRT control setpoint. By modulating open and closed, it controls secondary side pressure to the control setpoint value. The valve requires 40 seconds to stroke from fully open to fully closed. Because the capacity of the MSRT is nominally 50% of normal steam flow, the MSRCV needs to open only slightly to perform its cooldown function.

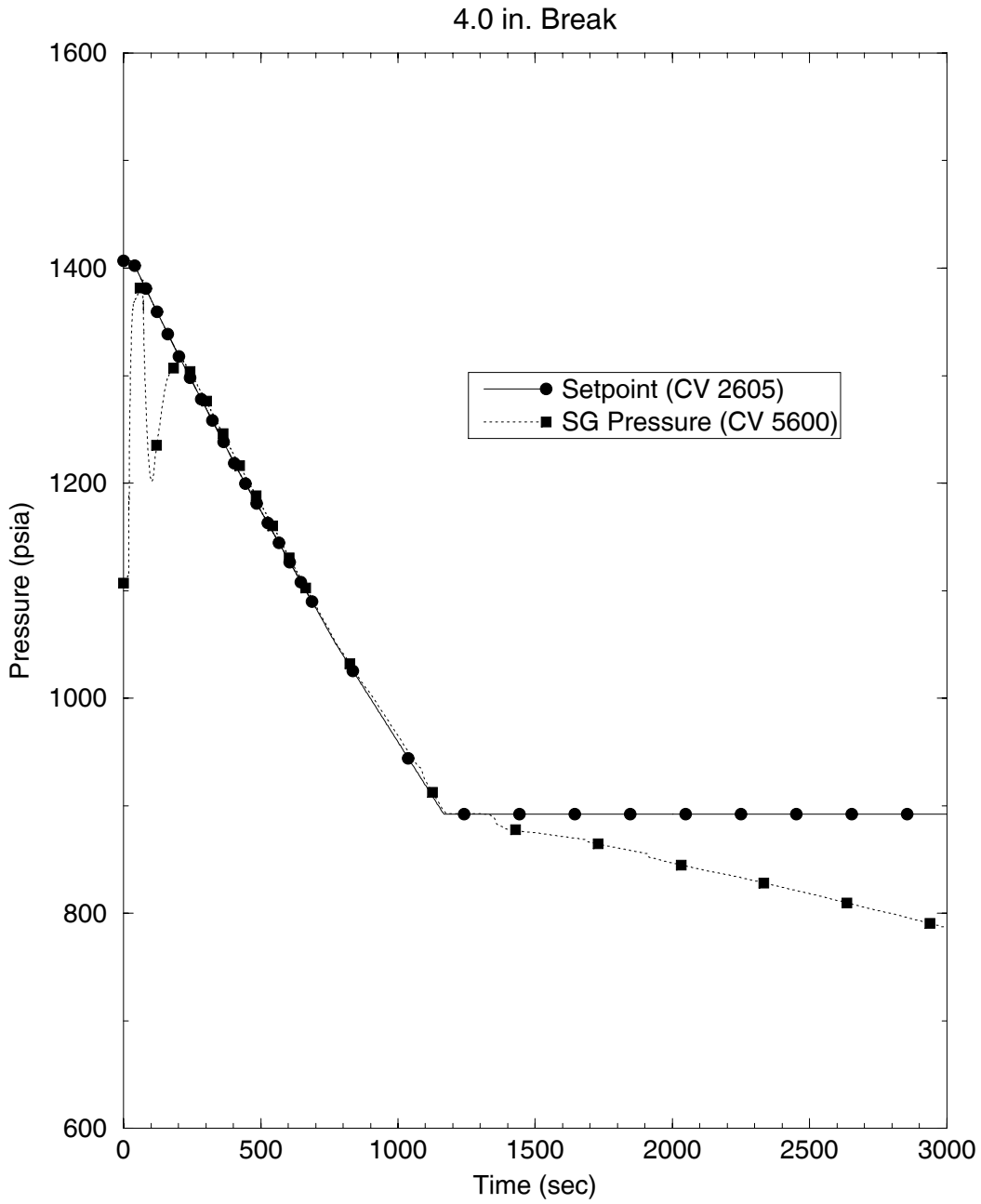


Figure 7-1 MSRT Response

RAI 8: *Section 5.2.2 of ANP-10263P addresses nodal changes because of length change but not sensitivity studies. Provide additional nodalization studies to justify the S-RELAP5 model for the economizer. The results of these studies will be used to justify the S-RELAP5 model to be used for licencing analyses.*

Response 8:

The original nodalization studies for the SG were performed for the ANF-RELAP methodology (ANF-89-151(P)(A), *ANF-RELAP Methodology for Pressurized Water Reactors: Analysis of Non-LOCA Chapter 15 Events*, May 1992). The resulting model was carried forward with minimal modification when the methodology was revised to use the S-RELAP5 code. The original model was that of a Combustion Engineering 2x4 plant.

The sample problem used 8 equal-length control volumes to model the active SG tubes. Each of these volumes had a length of approximately 6.7 ft, with the first 4 volumes oriented vertically upward and the next 4 oriented vertically downward. The U.S. EPR has longer tubes, so an additional node was added to both the upward and downward sides. Of the five upward oriented volumes, the first three (from the tubesheet to the top of the divider plate) each have a length of about 7.4 ft and the next two (from the divider plate to the centerline of the U bend) each have a length of about 7.1 ft. Therefore, the resulting U.S. EPR model has node lengths approximately equal to those in the approved model.

To verify the adequacy of the nodalization, the following studies will be performed. Component numbers refer to the loop 1 SG, but the changes will be made in all generators.

Case 1. Add heat structures to represent the metal in the economizer shell wall between the hot-side lower downcomer (component 512) and the cold-side lower downcomer (component 514). The structure will have an axial nodalization corresponding to the heights of the existing control volumes in the lower downcomer and boiler regions.

Case 2. Double the number of nodes in the active tube and boiler regions (components 124, 524, 526, 528-1, and 528-2) by dividing each control volume length and elevation change in half. Heat structures for the active tubes, the tube wrapper and the economizer shell added in Case 1 will be adjusted accordingly.

Case 3. Using Case 2 as a basis, double the number of nodes in the hot and cold side downcomers (components 512 and 514) by dividing each control volume length and elevation change in half. Heat structures for the tube wrapper and lower shell wall will be adjusted accordingly.

Each model will be run in steady-state mode initially and it will be verified that the model is steady. Appropriate transients will then be run to demonstrate the effect of each

change. The transients will include as a minimum, Increase in Steam Flow (SRP 15.1.3), Turbine Trip (SRP 15.2.2), and Loss of Normal Feedwater Flow (SRP 15.2.7).

Because the nodalization of the lower region of the SG in the U.S. EPR model is similar in scale to that in the approved non-LOCA methodology model, it is expected that these sensitivity studies will show that the existing model is adequate for U.S. EPR non-LOCA analysis. The sensitivity studies will be performed prior to submittal of the DCD.

NRC Comment

*The staff is not sure what to do with, or what is meant by, statements typical of page 5-16 of ANP-10263NP (**emphasis added**):*

*“The significant differences between the U.S. EPR U-tube SG design and current PWR U-tube SG designs are the increased size/volume of the unit and the incorporation of an axial economizer with a split downcomer and lower tube bundle region. The difference in size of the unit has no effect on the ability of S-RELAP5 to simulate the related hydrodynamic and thermodynamic phenomena. The fluid flow and heat transfer phenomena within the axial economizer region (single- and two-phase fluid flow, convection and nucleate boiling heat transfer) **are similar** to those in other regions of current PWR U-tube SG designs modeled using the Reference 5-1 methodology. Explicit modeling of the axial economizer geometry in the U.S. EPR S-RELAP5 SG model is allowed by the Reference 5-1 methodology (page 3-1) and **would be considered an acceptable plant-specific application of the currently approved methodology**. The Reference 5-1 methodology is suitable for analyzing U.S. EPR SG primary/secondary heat transfer phenomena during moderate overcooling events.”*

*Page 5-24 of ANP-10263NP (**emphasis added**):*

*“The fluid flow and heat transfer phenomena within the axial economizer region (single and two-phase fluid flow, convection and nucleate boiling heat transfer) **are similar** to those in other regions of current PWR U-tube SG designs modeled using the Reference 5-1 methodology. The MSLB SG model outlined in Reference 5-1 (a single SG boiler node with “steam-only” connecting junction to the steam dome) **is expected to remain** a conservative approach for calculating SG heat removal for the U.S. EPR SG since it forces all energy to be removed by conversion of the SG liquid inventory to steam, with no liquid release or carryover. Therefore, the Reference 5-1 methodology is suitable for analyzing U.S. EPR SG primary/secondary heat transfer phenomena during the pre-scrum period of MSLB events.”*

Page 5-26 of ANP-10263NP (**emphasis added**):

“U-tube SG with Axial Economizer: The MSLB SG model nodalization outlined in Reference 5-1 (a single SG boiler node with “steam-only” connecting junction to the steam dome) is expected to remain a conservative approach for calculating SG heat removal for the U.S. EPR SG since it forces all energy to be removed by conversion of the SG liquid inventory to steam, with no liquid release or carryover. The Reference 5-1 methodology is suitable for modeling the U.S. EPR SG heat transfer during an MSLB event.”

RAI 9: How will AREVA demonstrate that the current modeling approaches are actually representative of the U.S. EPR and remain conservative?

Response 9:

The approach consists of two elements: first, show that the U.S. EPR primary and secondary systems differ little from current operating PWRs in basic design, normal operating conditions and expected transient conditions. Due to similarity of the U.S. EPR primary and secondary system designs to current PWR designs, current modeling approaches apply to the U.S. EPR.

Secondly, the codes and analyses methodologies have a wide range of applicability to analyze reactor steady-state and transient conditions. Analysis methods have been developed, reviewed and approved for current PWR designs and operating conditions. U.S. EPR operating conditions are within the approved range of applicability of the methodology, and within the range of current PWR applications. Since the U.S. EPR design and operation falls within the ranges of hardware and conditions for which the analysis methodologies were developed and have been applied, the application of these methodologies to the U.S. EPR is appropriate. This will be demonstrated in the response to RAI 14.

Tables 2-1 and 2-4 of ANP-10263P compare U.S. EPR design parameters to current 4-loop PWR designs and to operating European PWR designs. The tables show that most U.S. EPR primary system design and operating parameters fall within the range of current operating PWRs. Parameters within the current range of PWR operation include: primary system pressure, most of the operating temperature range, average and maximum linear heat rates, average and maximum core heat fluxes, core average mass velocity and coolant velocity.

Exceptions are: core power, RCS loop flow, steam pressure and flow, RCS and pressurizer coolant volume, number of fuel assemblies and fuel assembly length, and steam generator secondary inventory. Each of these areas is discussed below.

U.S. EPR core power is higher than the power of current PWRs (although the average linear power density is lower). Higher power is achieved by increasing the number of

fuel assemblies in the core and the fuel assembly length, both of which increase the heat transfer area. Core heat transfer area is a plant specific input to the methodologies which does not affect the applicability or application range of the methodologies.

Increased loop flow and total core flow are necessary to support the power increase while maintaining fluid velocities and temperatures within the core and steam generators which are consistent with current plant operation. Likewise, because of the power increase, secondary system steam flow is also higher for the U.S. EPR than for current PWRs, and the secondary pressure is increased. However, core and steam generator flow areas are also increased so that the pressure drops and heat fluxes which depend on local fluid velocities in these components are within the typical range of current PWRs.

With regard to fluid volumes, the pertinent parameter to compare is the ratio of component fluid volume to reactor power. This RCS coolant volume to power ratio parameter is shown in Table 2-1 to be within the range of current PWRs. Pressurizer and steam generator volume-to-power ratios are higher than current PWRs. These increased water inventories improve system response to some transients.

The axial economizer in the secondary side of the steam generators is a change in hardware from the current PWR designs. This hardware separates the steam generator secondary into regions having somewhat different fluid temperatures during normal operation. For analyses, these regions are defined through input to the S-RELAP5 code which has the capability to calculate the fluid temperature variations. The demonstrated capability of calculating the appropriate steady-state for the U.S. EPR is a good indicator that these modeling changes appropriately represent U.S. EPR steam generators.

As with current PWRs, the U.S. EPR non-LOCA analyses are performed with codes and methodologies with demonstrated capability and appropriate ranges of applicability to perform these transients. The S-RELAP5 code is the principal tool for U.S. EPR non-LOCA analyses. This code incorporates features of the base RELAP5 program which provides general capability to model a wide variety of thermal-hydraulic systems containing water and steam, and to calculate steady-state and transient responses in these systems over a wide range of fluid conditions. (See Response to RAI 14.)

AREVA NP concurs that the writing style in the non-LOCA section of the report creates the impression in some statements that AREVA NP has reservations. This was unintended. We propose to review the section for statements such as "would be considered" and "is expected to" and strengthen them in the approved version of the topical report.

NRC Comment

Page 5-33 of ANP-10263NP:

“Steam generators with axial economizers: The U.S. EPR steam generator design features an axial economizer which channels the feedwater through the 180° sector of the downcomer and lower boiler regions that corresponds to the cooler, downflow legs of the U-tubes. However, modeling this feature is not warranted for a Main Steam Line Break analysis, in which all of a steam generator's downcomer and boiler regions are lumped together into a single volume and the feedwater is injected into the bottom of that volume.”

RAI 10: *This needs further clarification. Is the statement based simply on using the previous modeling approach or has it been, or will it be, demonstrated through sensitivity studies? What is done with the additional SG structures which form the economizer? Why is it not important to consider the economizer for this event?*

Response 10:

For the U.S. EPR, main feedwater is terminated early in the Main Steam Line Break (MSLB) transient and emergency feedwater is initiated. While main feedwater is injected directly into the top of the economizer, emergency feedwater is sprayed relatively high in the generator above the economizer structure. Both hot and cold sides of the downcomer receive emergency feedwater, thus effectively negating the effect of the economizer. This makes it unnecessary to model the economizer explicitly since it performs its function for only a very short period during the transient. Without the economizer, therefore, the generator is equivalent to those in typical Westinghouse or CE designs. The model used to analyze MSLB events in those plants will perform as well for the U.S. EPR.

The MSLB model for the U.S. EPR follows the approved methodology prescribed in Reference 10-1. The basis of the methodology is that fuel integrity (and primary loop integrity) is dependent on the heat removal rate from the primary. Conservative treatment of the break - allowing steam only out the break - maximizes the heat removal from the primary. This maximizes the reactivity impact of the cooldown, leads to the greatest probability of return to power, and maximizes the effect of the cooldown on the primary side level control system (pressurizer). From this perspective, the steam generator provides a boundary condition to the primary system.

As prescribed by the MSLB methodology, the steam generator (SG) secondary side fluid volume below the top of the primary steam separators is lumped in a single control volume. The fluid volume above this point is included in a second control volume (the steam dome), connected to the lower region by a junction that allows only steam to pass to the dome. This perfect separation of the liquid and vapor phases results in the removal of more energy from the steam generator than would occur if a two-phase

mixture were allowed to leave the steam generator through the break (if an explicitly modeled separator were used).

Using a single control volume to represent the lower portion of the SG is conservative for the MSLB analysis. The incoming cold feedwater is mixed with all of the liquid in the SG and produces a lower bulk secondary side fluid temperature than if the feedwater is mixed with only a portion of the SG liquid in a more complex nodalization that does not have the feedwater in contact with all of the fluid.

Sensitivity studies on the nodalization are not required because adding detail tends to impede cooldown associated with the simplified model. Note that the passive heat structures such as the SG shell wall, the tube wrapper, the tube divider plate, and the economizer shell are conservatively omitted from the model as these would release heat as the SG cools down, thus mitigating the temperature reduction.

Reference 10-1 – “SRP Chapter 15 Non-LOCA Methodology for Pressurized Water Reactors,” EMF-2310(P)(A) Revision 1, May 2004.

RAI 11: *It is not clear from the text or from Figure 2-4 what is meant by a variable cross-section area in the downcomer. Elaborate and include a discussion of any changes needed to ensure adequate two-dimensional (θ, z) nodalization of the downcomer for licensing analyses.*

RESPONSE 11:

Figure 2-4 of ANP-10263P shows a cross sectional view of the reactor vessel. The detail below (Figure 11-1) magnifies the region just below the cold leg inlet nozzle in the downcomer, showing the reactor pressure vessel (RPV) wall and the core barrel. The downcomer annulus is defined by the dimensions of these 2 boundaries.

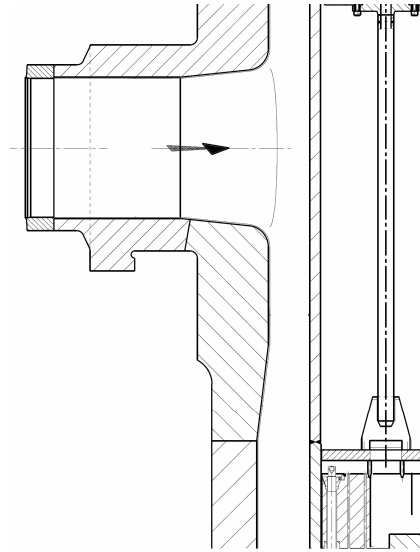


Figure 11-1 Detail of Reactor Vessel Inlet Nozzle Region of Downcomer

The cylindrical shell of the RPV consists of two sections, an upper and lower part. To minimize the number of large welds, which reduces the frequency of in-service inspections, the upper part of the RPV is machined from a single forging and fabricated with eight nozzles. Since the nozzles are fabricated into the massive plate used in the RPV shell, most of the reinforcement needed for the nozzle design is provided by the vessel material itself. Therefore, the nozzles used in this design are the “set-on” type requiring a less substantial weld bead than would otherwise be required.

Below the forging in the nozzle region, continuing down to the bottom of the downcomer, the lower RPV wall is thinner, resulting in an increase in the downcomer annular width. This change in the downcomer flow area is captured in the S-RELAP5 model.

The non-LOCA nodalization divides the downcomer into 6 axial regions. The region at the nozzle inlets and above there to the underside of the core barrel flange use BRANCH components, with the inlet nozzle region having a height equal to that of the outside diameter of the hot leg sleeves passing through the downcomer. The fluid volume in these regions is determined from the smaller RPV wall inner diameter at the nozzle forging.

Below the nozzles, the lower downcomer is divided into a 4-volume ANNULUS component. The uppermost control volume extends from the bottom of the inlet region to the elevation of the top of the active fuel. Two more equal length volumes extend to the elevation of the bottom of the active fuel, and the last volume to the bottom of the lower core support plate.

The uppermost volume in the lower downcomer spans the transition in the RPV inner diameter from 15.59 ft at the nozzles to 15.98 ft for the lower wall. The flow area of this control volume is calculated based on the actual dimensions of the wall above and below the transition and the distance below the nozzles where the transition in wall thickness occurs. The uppermost volume in the ANNULUS therefore has a smaller flow area than the 3 lower volumes.

In typical Westinghouse and Combustion Engineering designs, the transition (if any) of the vessel wall inner diameter from the nozzle belt region to the lower vessel wall is less pronounced and occurs closer to the nozzles, approximately at the node boundary defined at the bottom of the inlet region in the downcomer. In the modeling of those designs, the upper downcomer fluid volume is determined from the RPV inner diameter at the nozzle region and all four of the lower downcomer control volumes use the RPV diameter for the lower wall. An adjustment of the downcomer flow area in the upper ANNULUS node is not needed for these designs.

This modeling properly defines the flow area through the downcomer at the various elevations. This will result in the proper velocities and pressure changes as the coolant moves through the downcomer. The sole difference in the U.S. EPR model is that the lower downcomer does not use the same flow area in all four control volumes because of the elevation at which the RPV inner diameter transitions to the thinner wall.

RAI 12: *Is equation 2.51 in R1, "S-RELAP5 Models and Correlation Code Manual," correct? Should it be similar to Eq. 2.52? Is the term properly coded? (See RAI 2.10 response in EMF-2328(P).)*

RESPONSE 12:

Equations 2.51 and 2.52 are correct (from EMF-2100(P) Revision 4). This is demonstrated by the derivation presented below.

Equation 2.51 is derived from the total energy equation for the vapor space:

$$(M_n + M_v)U_g = M_vU_v + M_nU_n$$

where U_g , U_v , and U_n are the noncondensable-steam mixture, steam, and noncondensable specific internal energies, respectively, and M_v and M_n are the steam and noncondensable masses, respectively.

The definition of the noncondensable mass fraction is:

$$X_n = \frac{M_n}{M_n + M_v}$$

Dividing through by the noncondensable-steam mixture mass ($M_n + M_v$) and using the noncondensable mass fraction yields Equation 2.51:

$$U_g = X_n U_n + (1 - X_n) U_v$$

Equation 2.52 is derived from the Gibbs-Dalton assumption that the steam and the noncondensable occupy the same space:

$$M_n V_n = M_v V_v = (M_n + M_v) V_g$$

where V_n , V_v , and V_g are the noncondensable, steam, and noncondensable-steam mixture specific volumes, respectively. Dividing through by the noncondensable-steam mixture mass ($M_n + M_v$) and using the definition of the noncondensable mass fraction yields Equation 2.52:

$$V_g = X_n V_n = (1 - X_n) V_v$$

NRC Comment

A review of the informal PIRT discussed in the RAI responses in EMF-2328(P), suggested that the SG heat and mass transfer phenomena were ranked for the early phases (1, 2 and 3) of the SBLOCA and focused on loop seal clearing. In the U.S. EPR, SG mass and heat transfer is likely important to the later phases (4 and 5) as well.

RAI 13: *The referenced benchmarks (Table 4-2) do not specifically address SG mass and heat transfer. Expand the PIRT to specifically address SG mass and heat transfer during all phases, including phenomena associated with reflux condensation. Expand the validation data base for SG mass and heat transfer, including reflux condensation, particularly to address the later phases of the event.*

RESPONSE 13:

The informal SBLOCA PIRT considered only those phenomena that are ranked high. The phenomena that were ranked as medium or low were not listed and individual assessments were not identified for those phenomena. It is important to note that the SBLOCA model under discussion is an Appendix K model and not a realistic model. Therefore, consistent with the typical approach for Appendix K models, the conservatism associated with this deterministic model are intended to compensate for the lack of realistic modeling. Also, the rankings used in the Informal SBLOCA PIRT

are somewhat different than those used by Bajorek, et. al.¹, for a realistic SBLOCA. In this deterministic Appendix K application, the uncertainties of highly ranked phenomena have an influence on reportable PCT, and the effects of the phenomena are either bounded implicitly through model development or bounded explicitly through input modeling.

The phenomena that occur in the steam generators influence the PCT through timing of the transition from natural circulation to reflux condensation and timing of loop seal clearing. The assessments performed show that S-RELAP5 is in acceptable agreement with the measured data. However, since the uncertainties were not quantified, a bias was used to bound the effects of the phenomena on PCT. The method used to bound the uncertainties was to model the RCS loops independently with a nodalization that promotes the conditions which cause the broken loop and an adjacent intact loop to remain plugged for the limiting break size. This procedure will result in a significantly higher PCT than if the broken loop was allowed to clear. With the significantly higher PCT from this process, the uncertainties associated with the phenomena occurring in the steam generator are bounded and do not require additional consideration.

Since the U.S. EPR steam generator has an economizer and a partial cooldown controller, additional assessments might be required if the phenomena associated with these two features were significantly different from existing PWR designs. The SBLOCA limiting break from ANP-10263(P) will be examined below to determine if the phenomena occurring in the steam generators differs significantly from either existing PWR designs or the current code assessment cases. Figure 13-1, which corresponds to Figure C-6 on page C-18 of ANP-10263(P), shows the primary and secondary pressure histories from the U.S. EPR SBLOCA sample problem along with vertical dashed lines showing the demarcations defined by the periods of a SBLOCA. The blowdown period ends when the primary pressure decreases to just above the steam generator pressure and then starts following the secondary pressure. This occurs at approximately 45 seconds. The natural circulation period extends from 45 seconds until 300 seconds where liquid ceases to flow to the descending side of the steam generator tubes and reflux condensation dominates the ascending side. The venting of the steam from the loop seal clearing process allows the core mixture level to recover to the elevation of the cold legs which occurs at 555 seconds. The boil-off period extends until the minimum core mixture level, occurring at 1073 seconds, and is followed by the recovery period. Figure 13-1 will be used to assess the phenomena occurring in the steam generator during the SBLOCA boil-off and recovery periods for ranking the partial cooldown in terms of mass and heat transfer. Figure 13-2, the economizer temperature histories during the SBLOCA along with the period demarcations, will be used to assess

¹ S. M. Bajorek, A. Ginsberg, D. J. Shimeck, K. Ohkawa, M. Y. Young, L. E. Hochreiter, P. Griffin, Y. Hassan, T. Fernandez, D. Speyer, "Small Break Loss of Coolant Accident Phenomena Identification and Ranking Table (PIRT) for Westinghouse Pressurized Water Reactors", Ninth International Topical Meeting on Nuclear Reactor Thermal Hydraulics (NURETH-9), San Francisco, California, October 3-8, 1999.

the phenomena occurring in the steam generator during all periods of the SBLOCA for ranking the economizer in terms of mass and heat transfer.

Figure 13-1 shows the effects of the partial cooldown, which started just after 200 seconds and continues past 1100 seconds. At the end of loop seal clearing, the break flow transitions from low quality two-phase flow to primarily steam flow which causes the primary system to depressurize at an increased rate. The higher depressurization rate of the primary system causes the primary pressure to decrease below the secondary pressure at about 760 seconds. After this time, condensation in the steam generators ceases since the secondary temperature will be superheated with respect to the primary saturation temperature. Except for the decreasing pressures from the partial cooldown, the process is identical to those found in current PWR designs. Since mass transfer and reflux condensation in the steam generator during the boil-off and recovery periods are currently ranked as medium low importance, no change in ranking is warranted. Also, the current assessments are sufficient since no new phenomena are occurring.

The effect of the economizer is to lower the steam generator outlet temperature, which improves the plant efficiency during normal operating conditions. Figure 13-2 shows the calculated temperature histories of the bottom nodes on the hot and cold sides of the economizer. Immediately after break initiation, both temperatures rise in response to the cessation of main feedwater flow and the main turbine stop valve closure. A distinct temperature difference is maintained until 240 seconds. After 240 seconds, the hot and cold side temperatures coincide until the PCT node quenches after 1300 seconds, which is the result of the partial cooldown that was started at approximately 200 seconds. After 240 seconds, the economizer behaves the same as existing PWR designs through the loop seal clearing, boil-off, and recovery periods of a SBLOCA. Since the pumps finally coastdown by 150 seconds, the economizer has no influence during the blowdown period and the first 105 seconds of the natural circulation period. Finally, the only period of influence by the economizer is a small time frame during the natural circulation period. Since natural circulation flow ceases after 300 seconds, the economizer had little influence on flow between 150 seconds and 240 seconds. Consequently, the economizer has no impact on the current steam generator rankings in the Informal SBLOCA PIRT.

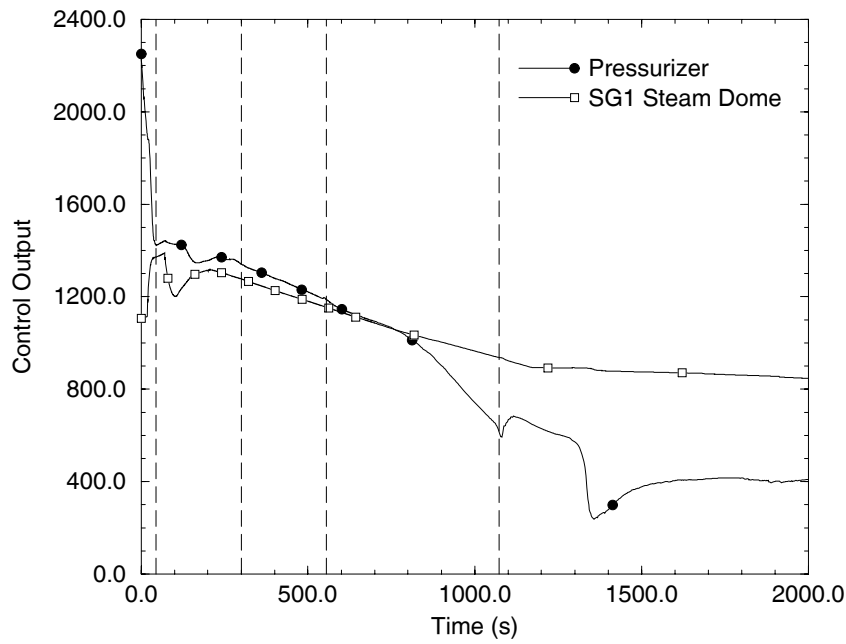


Figure 13-1 Primary and Secondary System Pressures for 4 Inch Break

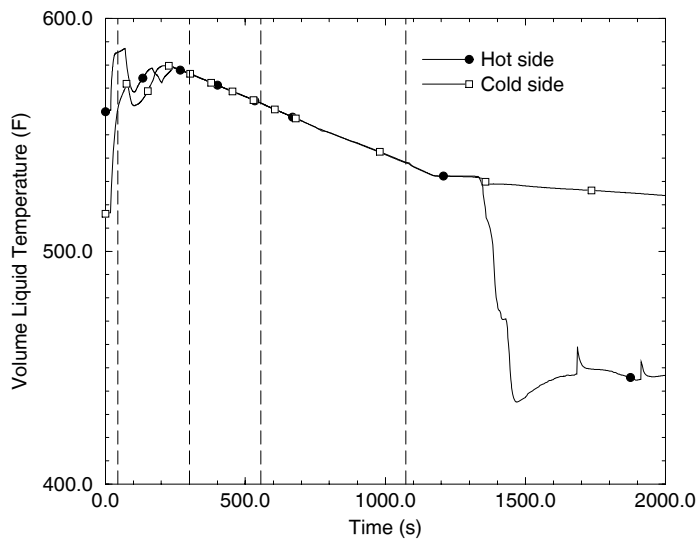


Figure 13-2 Steam Generator 1 Liquid Temperatures in the Economizer for 4 Inch Break

NRC Comment

In addition to the larger RCS component volumes and SG component volumes, the U.S. EPR operates at a higher power level, with higher RCS temperatures and higher SG pressures than the typical U.S. PWR designs for which S-RELAP5 was previously accepted.

RAI 14: *Verify that the mass and heat transfer correlations in S-RELAP5 adequate cover the ranges for the anticipated increases in the mass and energy transfer rates expected in the U.S. EPR, for both small break LOCA (including SGTR) and non-LOCA accidents.*

RESPONSE 14:

S-RELAP5 has the capability to analyze water-containing systems over a wide range of conditions. For example, S-RELAP5 contains a representation of the 1967 ASME steam tables which provide accurate fluid conditions which may range from the freezing point of liquid water to the critical point of a steam-water mixture. Fluid flow and pressure drops can be computed for both laminar and turbulent flow conditions and for both single-phase and two-phase fluid conditions. This capability encompasses the full range of expected PWR and U.S. EPR steady-state and transient conditions.

Initial heat generation is input to the code, and heat transfer rates are typically calculated based on correlations appropriate for the local fluid and flow conditions. The range of applicability includes that associated with the correlation being applied and extrapolations and interpolations which have been demonstrated as appropriate to extend the correlations and to interface regime changes. Details of the flow regime and heat transfer modeling are given in the S-RELAP5 Models and Correlations Code Manual, EMF-2100(P).

A summary of many of the S-RELAP5 heat transfer correlations, the regime of application, and ranges of applicability is given in the response to RAI 2 on the realistic LOCA methodology, EMF-2103(P). This response, however, is specific to LBLOCA conditions and focuses almost entirely on post CHF heat transfer. For non-LOCA transients, pre-CHF heat transfer is dominant. The pre-CHF heat transfer regimes encountered are convection to liquid water and nucleate boiling.

For turbulent flow, single-phase convection heat transfer to liquid is calculated using the Dittus-Boelter correlation with a minimum Nusselt Number of 7.86. Laminar and natural circulation flow conditions are also considered by incorporating a natural circulation correlation to provide a floor or minimum value of the turbulent flow heat transfer coefficient. The quoted range of applicability of the Dittus-Boelter correlation from Kreith is:

$$\begin{aligned} \text{Re} &> 6000 \\ 0.7 &< \text{Pr} < 160 \\ \text{L/D} &> 60 \end{aligned}$$

The natural convection correlation has two regions:

$$\begin{aligned} &Gr_f Pr_f < 10^9 \\ \text{and } 10^9 &\leq Gr_f Pr_f \leq 10^{13} \end{aligned}$$

The forms of the Dittus-Boelter correlation and the natural circulation correlation are theoretically derived and only the correlation coefficients and exponents are experimentally determined and limit the range of applicability. The Dittus-Boelter correlation has been widely used and shown to have applicability even beyond its quoted range. Applicability of these combined correlations should encompass single-phase, forced convection conditions experienced in PWR non-LOCA transients. The combined correlation will apply throughout the primary system for both steady-state and transient non-LOCA conditions.

Nucleate boiling heat transfer, flow of a two-phase mixture, and single-phase steam flow occur in the secondary side of PWR steam generators and steam lines and in the core during a small break LOCA. The treatment of nucleate boiling by S-RELAP5 is described in EMF-2100(P), and uses the Chen correlation. The range of conditions for which the Chen correlation was derived is given in the Question 2 RAI response to the realistic LOCA methodology report EMF-2103(P) as:

$$\begin{aligned} \text{Pressure} &< 510 \text{ psia} \\ \text{LHGR} &< q_{\text{CHF}} \\ \text{Core inlet mass flux} &< 200 \text{ kg/s-m}^2 \end{aligned}$$

Other investigators have extended this correlation to systems with higher pressures and shown that the correlation adequately predicts nucleate boiling heat transfer for pressures in the range of 1000 psia. Code prediction of observed steady-state conditions in the steam generators is further proof that the code and correlations are valid for calculating secondary heat transfer.

Applicability of Other Approved Methodologies to U.S. EPR Design

RAI 15: *The COPERNIC code demonstrated that the LOCA initial conditions were not necessarily limited in the beginning of life depending on the power histories. Please assess the situation for the EPR.*

RESPONSE 15:

The topical report ANP-10263P addresses only SBLOCA. Hence the response to this RAI pertains only to SBLOCA applications.

The COPERNIC code is not used to determine fuel conditions for SBLOCA analyses. The methodology approved in Reference 15-1 utilizes the RODEX2 code to calculate burnup-dependent, initial fuel rod conditions for each active core region in S-RELAP5.

Initial fuel rod stored energy is not a significant parameter for SBLOCA since the stored energy is removed early in the event when reactor scram occurs. The SBLOCA analysis simulates End-of-Cycle (EOC) conditions due to the dominant effect of a top-skewed axial power profile, as well as a larger actinide decay heat at EOC. The RODEX2 code is used to predict the initial fuel rod conditions at EOC for use in the S-RELAP5 calculation. The actual power history used in the RODEX2 code to predict fuel rod conditions at EOC does not have a significant effect on the PCT.

Reference 15-1 – PWR Small Break LOCA Evaluation Model, S-RELAP5 Based, EMF-2328(P)(A), Revision 0, March 2001.

RAI 16: *The maximum rod gas pressure is limited to below a value which would cause (1) the fuel cladding gap to re-open, and (2) extensive departure from nucleate boiling (DNB) propagation to occur. Does this imply that EPR allows for certain DNB failures and propagation?*

RESPONSE 16:

The current NRC approved topical report (BAW-10183P-A) allows for certain DNB failures and propagation. The treatment for the U.S. EPR will be consistent with this topical report.

The core protection calculations will be repeated for the U.S. EPR in accordance with the existing NRC approved methodology. Under normal and design operating conditions, application of the methodology will result in no additional failed fuel rods due to simultaneously being above system pressure and experiencing DNB. The limiting analysis with simultaneous peaking and burn-up limits will be performed with a protection criterion of either 99.99% of the rods not failing or one failed fuel pin per core quadrant, whichever is most limiting.

Core Neutronics

RAI 17: *Page A-1 of ANP-10263P discusses the subject of “Reflectors.” Since this a new reflector design, will there be a separate topical report addressing the new design?*

RESPONSE 17:

AREVA NP does not intend to issue a separate topical report for the Heavy Reflector. The Heavy Reflector will be described in the U.S. EPR DCD. As discussed in ANP-10263P, Section A.1.0, the neutronics treatment of the Heavy Reflector is similar to that used for the standard shroud reflector. In both cases, transport theory calculations are performed to generate a set of equivalent reflector cross sections. The reflector cross sections are then used with the PRISM reactor nodal code for the generation of 3D power distributions and reactivities. The process used to generate the reflector cross sections used in the Harris, Gravelines 5 Unit 1, GKN-1 and GKN-2 benchmarks is similar to the process used to generate the reflector cross for the Heavy Reflector. Additionally, MCNP calculations were performed and compared to the equivalent PRISM cases. These comparisons were used to obtain adjustment factors to be applied to the Heavy Reflector cross sections used in the U.S. EPR PRISM models. The neutronics behavior of the Heavy Reflector is understood and modeled through first principles in the same manner that the standard reflectors are treated.

RAI 18: *Page A-15 of ANP-10263P, section A.2.3, presents the methodology description and the validation process associated with these methodologies. However, no technical basis was provided to support these applications. For example, in sub-section A.2.4.1, it is simply stated that the critical experiments provided in SAV95 are still valid. No reason was given as to why they are still valid. Provide this justification.*

RESPONSE 18:

The design methodology to be applied to the U. S. EPR is identical to that described in Reference A-1 with the sole exception of using a 0.625 eV cross section cutoff rather than a 1.855 eV cutoff. This only impacts the 2 group PRISM calculations. The results presented in Reference A-1 which are dependent on this difference have been reanalyzed and the results are presented in ANP-10263P, specifically the B&W Critical experiments, core follow comparisons, and startup physics test comparisons. The critical experiment measurements which were provided for SAV95 in Reference A-1 Section 4.1 remain valid since the cross section generator MICBURN-3/CASMO-3 combined with the modified K library are unchanged.

RAI 19 *Page A-26, Section A.3.0, Power Distribution Uncertainties for POWERTRAX/S, and subsequent sub-sections, allude to a new power distribution calculational method and uncertainties determination. The last sentence of the first paragraph in this section, states that this methodology will be discussed in a future topical. Will this be a separate topical to the DCD? What is the time-line for this topical? Additional discussions may be required.*

RESPONSE 19:

A new measured power distribution calculation method will be used. The methodology is described in Section A.3.0 and a discussion will also be included in a separate topical report on setpoint safety analysis methods where the measured power distribution is applied.

The method used to determine the uncertainties associated with the measured power distribution is the same as that described in Reference A-3 and further used in Reference A-1. The results of the uncertainty analyses using this methodology will also be included in the setpoint safety analysis methods topical report.

***RAI 20:** On page A-33, Sub-Section A.3.3.2, the subject of Local Peaking Factor Uncertainty is discussed. The remain text of this sub-section and sub-sequent section provide the staff with the results of the uncertainties for the respective sections. However, the statistical method used to arrive at these results is not discussed. Please provide the statistical methodology used to arrive at these values, as well as references.*

RESPONSE 20:

In Section A.3.3 it is stated that the method used to determine the local peaking factor uncertainty is the same as that described in Reference A-3. This statistical method was further used in Reference A-1 and described by referring to Reference A-3. The statistics are derived from six assembly lattices, three of which contain gadolinia fuel.

In Section A.3.3.2 it was stated that “Only UO₂ pin powers were used for the LPF (Local Peaking Factor) uncertainty component because the very low gadolinia pin powers skewed the statistics when differences were converted to percentages. However, the gadolinia pin power differences did behave similarly to the UO₂ pin power differences. As the gadolinia burns out the gadolinia pin power percent differences would be expected to behave like the UO₂ pin power percent differences.”

The uncertainties for the gadolinia-bearing assemblies are larger than those for the non-gadolinia-bearing assemblies. Therefore, as in References A-1 and A-3, the uncertainties are conservatively derived from the three lattices which contain gadolinia fuel.

Heavy Reflector in Place of Core Barrel Thermal Shield Pads**NRC Comment**

In sections 4 and 5 of the topical report, the following description is provided:

The effect of the metal in the reflector will be represented by standard heat conductors, and the bypass flow through coolant flow channels present in the reflector metal structure will be simulated by suitable standard flow paths.

- RAI 21:** a) *Please describe the coolant flow system for these channels (number and size of the channels, and flow path from entrance to exit).*
- b) *Please provide the AREVA plans to validate the flow path modeling. Include a discussion on the entrance/exit loss factors, channel pressure drop, likelihood and consequences of steam binding (or blockage) in some or all channels, and the adequacy of the fluid flow map to model the expected flow pattern in the channels. How does blockage of these channels affect the EPR performance for AOOs, DBAs, LOCAs (large and small) and long term cooling?*

RESPONSE 21:

The space between the multi-cornered radial periphery of the reactor core and the cylindrical core barrel is filled with a stainless steel structure, called the heavy reflector, the purpose of which is to reduce fast neutron leakage and flatten the power distribution. The reflector is inside the core barrel above the lower core support plate. To avoid any welded or bolted connections close to the core, the reflector consists of stacked forged slabs (rings) positioned one above the other with keys, and axially restrained by tie rods bolted to the lower core support plate. (See Figure 21-1.)

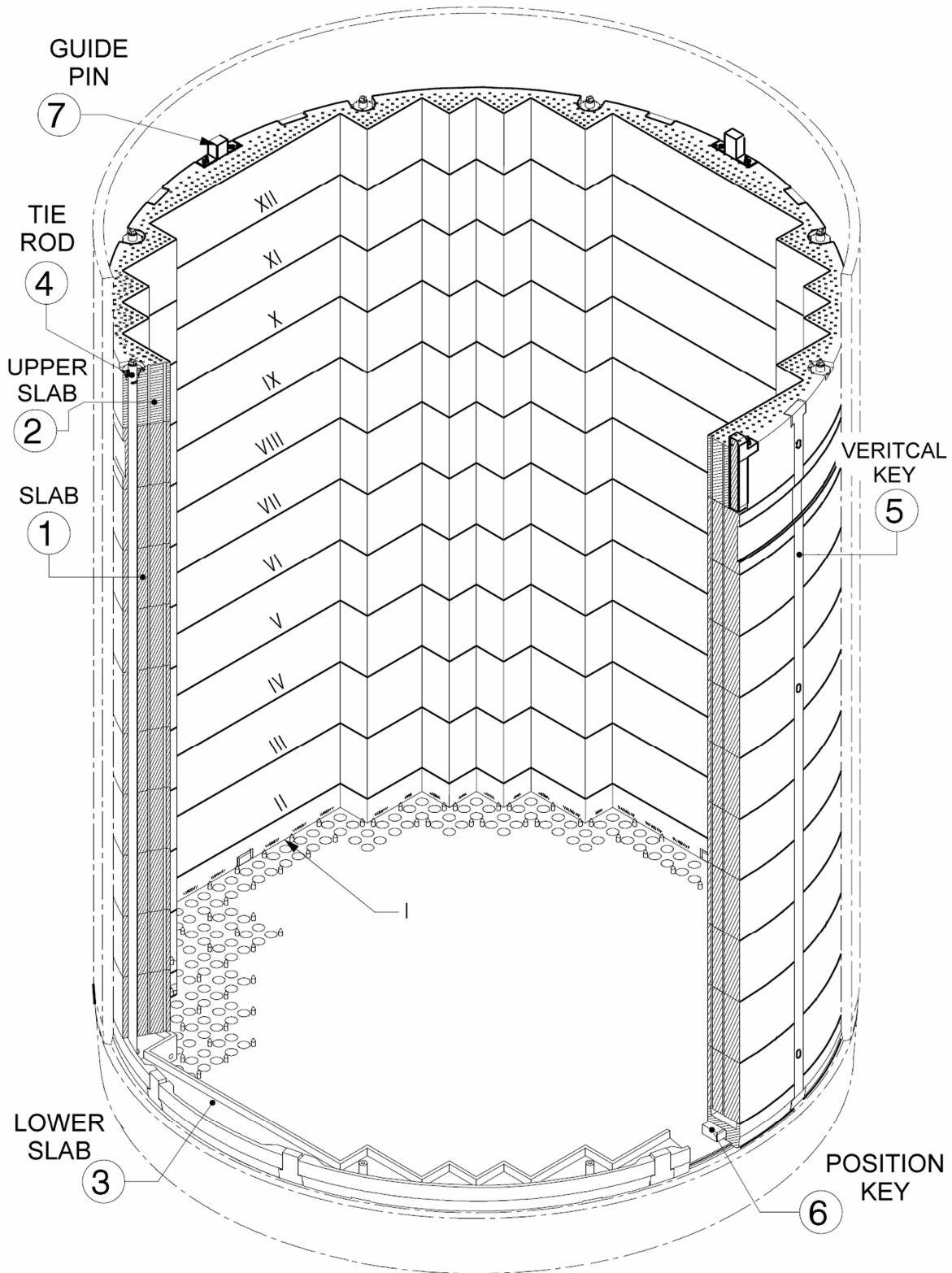


Figure 21-1 Heavy Reflector

The heavy reflector is dimensioned to accommodate expansion of the fuel assembly arrangement. Water cooling is provided by means of coolant channels inside the heavy reflector to prevent excessive stress and deflections of the rings due to the heat generated inside this steel structure by absorption of gamma radiation.

The coolant channels consist of 784 holes (approximately 0.5 inch diameter) running axially through each ring of the heavy reflector. These align with holes in adjacent slabs, creating a core bypass flow path from the lower plenum to the upper plenum. This is analogous to the bypass path through the core baffle or core shroud region in typical Westinghouse or CE designs. The principal hydraulic difference is that in the U.S. EPR, this region surrounding the core inside the core barrel is approximately 95% metal with 5% water, while in conventional designs this ratio is reversed. The flow rate through the heavy reflector is 1.24% of the total RCS flow, compared to a range from 0.5% to 1.7% for various Westinghouse and CE plants.

The S-RELAP5 model of the HR core bypass region consists of a 2-node (or 3-node in the SBLOCA model) vertical PIPE component to model the flow path through the cooling holes, and two heat structures to model the metal mass of the reflector itself.

As a modeling simplification to achieve the proper junction elevations, the heavy reflector is assumed to have the same height as the active core. The gross volume of a right circular cylinder contained within the core barrel bounded by the active core elevations is obtained and the cross-sectional area occupied by the core (from the assembly pitch squared times the number of assemblies) times the active core height is subtracted from the gross volume. Using the mass of all of the structural material in the heavy reflector (slabs, tie rods, vertical keys, and miscellaneous parts), the volume occupied by the heavy reflector structure is obtained by dividing by the density of the stainless steel material. This metal volume is subtracted from the gross volume of the region resulting in a net fluid volume consisting of the flow holes, the annular space between the heavy reflector and the core barrel and the space between the heavy reflector and the core periphery. The net fluid volume is evenly distributed to the control volumes in the PIPE component representing the heavy reflector bypass region.

A hydraulic diameter for the heavy reflector bypass region is approximated from the region flow area and the wetted perimeter of the core barrel, outer heavy reflector surface and the perimeter of all the holes. The form loss for the junctions at the entrance (from the lower reactor vessel plenum) and exit (to the upper plenum) of the heavy reflector region are estimated from an assumed pressure drop and from abrupt area change relationships. These loss coefficients are adjusted to obtain the target value of 1.24% of the total RCS flow rate through the region.

The metal mass of the heavy reflector is also represented in passive, cylindrical heat structures connected to the core region and to the heavy reflector bypass region. To model this structure, the total mass of the reflector is divided into two concentric hollow

cylinders. The inner cylinder is connected to each of the active core hydrodynamic volumes at its inner radius and to the heavy reflector bypass flow path at its outer radius. The outer half of the mass in the second cylinder has a connection to the reflector bypass path at both its inner and outer radii.

The inner structure is divided into the same number and length of axial nodes as is the active core region. The left side of each axial node in the structure is connected to an active core hydrodynamic volume, preserving the area of the heavy reflector at the core interface. The right side of each axial node is connected to one of the PIPE volumes in the heavy reflector region. This is similar to the modeling used for the core baffle plate or core shroud heat structure in conventional plants, except that the latter uses rectangular geometry for the structure.

The effective inner diameter of the heavy reflector material is found from the metal volume of the reflector divided by the length of the active core to give an effective cross-sectional area. With this area and the outer diameter assumed to be that of the core barrel ID, this can be solved for an effective inner diameter. The effective thickness of the metal in the annular region is half of the difference in the inner and outer diameters. This thickness is divided by 2 to give the dimensions of the two concentric cylinders representing the heavy reflector metal.

The outer portion of the reflector is also modeled with a cylindrical heat structure, but is simpler as both sides are in contact with the heavy reflector bypass region. The axial length is divided into segments corresponding to the PIPE node lengths. This is analogous to the modeling used for the former plate heat structure in the core baffle or shroud regions of conventional plants.

The resulting model is nearly identical to that used in the approved methodology models. The differences lie in the amount of fluid within the region and the details of the heat structures to model the metal structure.

The likelihood of steam binding in the heavy reflector bypass path is negligible. The heat flux from the core is not sufficient to vaporize the fluid in the heavy reflector region, even for the most severe non-LOCA events. Were it to occur, blockage of the flow holes would only increase the flow through the active core region, thus increasing the margin to DNB. When the region is voided due to LOCA blowdown, it behaves the same as the core baffle or shroud region in a conventional plant. The purpose of the flow path through the holes is to cool the metal in the massive heavy reflector slabs. A loss of cooling could possibly result in some deflection of the metal rings in the heavy reflector, but would not have a detrimental effect on accident analysis.

General Comment

RAI 22: *On page 2-24 of the ANP-10263P, sub-section 2.2.4.2.1 discusses the subject of the "Aeroball System." Does AREVA intend to submit this methodology for NRC Staff approval prior to the submittal of the DCD?*

RESPONSE 22:

The Aeroball System will be described in the DCD. Consistent with past industry practice, the power distribution measurement uncertainty associated with the Aeroball System will be submitted for NRC review and approval as part of the topical report on setpoint safety analysis methods (See Response 19).

The Aeroball System is an offline measurement system used to verify that the core is operating within expected parameters. Data obtained from the Aeroball System will also be used to calibrate the SPNDs and the excore detectors. The function of the Aeroball System is consistent with that of the moveable incore detector systems currently employed in the U.S. Additional information concerning the Aeroball System can be found in ANP-10271P.

Further details of the use of the POWERTRAX/E code to calibrate the incore SPNDs to the Aeroball results will be discussed in the topical report on setpoint safety analysis methods.

RAI 23: *In an SBLOCA, the RCS begins to depressurize and about 30 minutes later two-phase natural circulation is lost. Reflux condensation cooling begins and a slug of unborated water is formed in the descending half of the SG U-tubes, in the crossover leg, in the pump volume and possibly in the lower plenum of the vessel. Later this slug could be transported to the core in several ways. This transient is an important issue (Generic Safety Issue 185). How will GSI 185 be addressed for the U.S. EPR?*

RESPONSE 23:

The importance of GSI 185 is recognized. This issue is not part of the topical report ANP-10263P. The issue will be addressed in the U.S. EPR DCD submittal.

NRC Correspondence References:

- R1. "S-REALP5 Models and Correlations Code Manual," EMF-2100(P) Rev 4, May 2001.
- R2. ISP-27, "BETHSY Experiment 9.1.B - 2" Cold Leg Break Without HPSI and With Delayed Ultimate Procedure," November 1992, OECD/NEA/CSNI/R(92)20.

- R3. *“PWR Small Break LOCA Evaluation Model, S-REALP5 Based,” EMF-2328(P), January 2000.*
- R4. *“BETHSY Nodalization Study During Mid-Loop Operation,” V. Segon, et al., International Conference, Nuclear Energy in Central Europe 2001, September 10-13, 2001.*
- R5. *“Heat Transfer Characteristics of Reflux Condensation Phenomena in a Single Tube,” G-H. Chou, J-C. Chem, Nuclear Science and Engineering: 127, 220-229 (1997).*
- R6. *“Non-uniform flow distribution in steam generator U-tubes of a pressurized water reactor plant during single- and two-phase natural circulation,” J-J. Jeong, et al., Nuclear Science and Engineering: 231, 303-314 (2004).*
- R7. *“Nonuniform Steam Generator U-Tube Flow Distribution During Natural Circulation Tests in ROSA-IV Large Scale Test Facility,” Y. Kukita, et al., Nuclear Science and Engineering: 99, 289-298 (1988).*
- R8. *“Intentional Depressurization of Steam generator Secondary Side during a PWR Small-Break Loss-of-Coolant Accident,” H. Asaka, Y. Hukita, Journal of Nuclear Science and Technology: 32[2]. pp. 101-110 (February 1995).*
- R9. *“Thermal-hydraulic characteristics of a next generation reactor relying on steam generator secondary side cooling for primary depressurization and long-term passive core cooling,” Nucl. Eng. Design, 185, pp. 83-96, (1998).*
- R10. *“Reflux condensation behavior in a U-tube steam generator with or without noncondensables,” Tay-Jian Liu, Nuclear Engineering and Design, Volume 204, Issues 1-3, February 2001, Pages 221-232.*
- R11. *“Reflux condenser mode with non-condensable gas: assessment of Cathare against Bethsy test 7.2C,” B. Noel and R. Deruaz, Nuclear Engineering and Design, Volume 149, Issues 1-3, 1 September 1994, Pages 291-298.*
- R12. *BETHSY Test 9.113. ISP-27, Clement, P., Chataing, T., Deruaz, R., OECD/NEA/CSNI/R(92)20, (1992).*

Bibliography

Single Tube Tests

Lee, K. W., et al., *“Local heat transfer during reflux condensation mode in a U-tube with and without noncondensable gases,” Int. J. Heat Mass Transfer, Vol. 49, pp. 1813-1819, (2006).*

Girard, R., and Chang, J. S., "Reflux condensation phenomena in single vertical tubes," Int. J. Heat Mass Transfer, Vol. 35, pp 2203, (1992).

Multi-tube Tests

Loomis, G. G., and Soda, K., "Results of the Semiscale MOD-2A natural circulation experiments," NUREG/CR-2335, (1982).

Kukita, Y., Nakamura, H., and Gotou, H., "Nonuniform steam generator U-tube flow distribution during natural circulation tests in ROSA-IV large scale test facility," Nucl. Sci. Eng., 99, pp. 289-298, (1988).

Dumont, D., et al., "Loss of residual heat removal during mid-loop operation: BETHSY experiments," NURETH 6, Grenoble, (1993).

K. Umminger, R. Mandl and R. Wegner, "Restart of natural circulation in a PWR-PKL test results and 5 calculations," Nuclear Engineering and Design, Volume 215, Issues 1-2, June 2002, Pages 39-50.

Large Scale Separate Effects Tests

Howard, R. C., et al., "PWR FLECHT SEASET Steam Generator Separate Effects Task Data Report," NUREG/CR-1366, (1980).

Howard, R. C., and Hochreiter, L. E., et al., "PWR FLECHT SEASET Steam Generator Separate Effects Task Data Analysis and Evaluation Report," NUREG/CR-1534, (1982).

Additional SG Heat Transfer Tests for SBLOCA Qualification

Klaus Kochshkamper, "Validation of the Thermal-Hydraulic Computer Code S-RELAP5 for Performing Loss-of-Coolant Accident Analysis (LOCA) in Pressurized Water Reactors (PWRs)," Nuclear Society of Slovenia, 2nd Regional Meeting: Nuclear Energy in Central Europe, 11-14 September 1995. (LOFT L2-5, PKL III B.2 and BETHSY 6.2)